https://doi.org/10.5194/tc-2023-43
Preprint. Discussion started: 4 April 2023

The Cryosphere Discussions

Reconciling ice dynamics and bed topography with a versatile and fast ice thickness inversion

Thomas Frank[1], Ward J. J. van Pelt[1], and Jack Kohler[2]

[1]Department of Earth Sciences, Uppsala University, Uppsala, Sweden
[2]Norwegian Polar Institute, Fram Centre, Tromsø, Norway

Correspondence: Thomas Frank (thomas.frank@geo.uu.se)

Abstract. We present a novel thickness inversion approach that leverages globally available satellite products and state-of-the-art ice flow models to produce distributed maps of subglacial topography independent of bed observations. While the method can use any complexity of ice physics as represented in ice dynamical models, it is computationally cheap, enabling applications both on local and large scales. Using the mismatch between observed and modelled rates of surface elevation change (*dh/dt*) as the misfit functional, iterative pointwise updates to an initial guess of bed topography are made, while mismatches between observed and modelled velocities are used to simultaneously infer basal friction. The final product of the inversion is not only a map of ice thickness, but a fully spun-up glacier model representing the dynamic state of a given glacier. We here present the method, and use an artificial ice-cap built inside a numerical model to test it and conduct sensitivity experiments. Even under a range of perturbations, the method is stable and fast. Finally, we apply the approach to the tidewater glacier Kronebreen on Svalbard. Ultimately, our method shown here represents a fast way of inferring ice thickness where the final output forms a consistent picture of model physics, input observations and bed topography.

1 Introduction

Knowledge of the ice thickness of glaciers is crucial for a range of applications, from field work planning, to water management and ultimately for projections of expected sea level rise in the face of climate warming (Oppenheimer et al., 2019; Rounce et al., 2023). Ice thickness not only determines the ice volume of a glacier, but the subglacial topography is furthermore a key control on future retreat of glaciers. As such, accurate bed maps are instrumental to initialize prognostic simulations of numerical ice flow models with the correct boundary conditions.

Ice thickness can be established using geophysical methods such as ground-penetrating radar (Bogorodsky et al., 1985). However, observations are only dense along their acquisition lines, while considerable spacing between lines is the norm. To produce distributed maps of ice thickness, statistical techniques have been developed to interpolate between observations

https://doi.org/10.5194/tc-2023-43
Preprint. Discussion started: 4 April 2023

(Flowers and Clarke, 1999; Fretwell et al., 2013; Neven et al., 2021). However, only a small fraction of glaciers worldwide have any thickness observations at all (Welty et al., 2020).

As an alternative to field measurements, inversion techniques have been introduced that allow to derive a bed estimate from easily-obtainable surface observations alone. Early works include the use of scaling relationships that allow the computation of mean bed elevation from surface area (i.e. volume-area scaling, Chen and Ohmura (1990); Bahr et al. (1997, 2014)). More advanced approaches apply computational methods relying on a physical understanding of how ice flows, often (when available) in conjunction with measured ice thicknesses. The underlying rationale is that easily observable surface characteristics, such as the surface elevation height, are a product of the external climate forcing (e.g. climatic mass balance), ice dynamics and the subglacial topography, and therefore an inference about the latter can be made from knowledge of the previous. The recent years have seen an increasing amount of such new ice thickness inversion approaches; an overview of widely used methods is given in Farinotti et al. (2017, 2021). The large majority of approaches follow at least one of the two strategies: in the first, the physical calculations of ice dynamics underpinning the inversion are conducted along flow-lines or at randomly selected points on a glacier, and subsequently the results are extrapolated to surrounding areas, often while taking into account some first-order glaciological principles, e.g. the strong link between surface slope and ice thickness (Farinotti et al., 2009; Linsbauer et al., 2009; Huss and Farinotti, 2012; Li et al., 2012; Linsbauer et al., 2012; Paul and Linsbauer, 2012; Clarke et al., 2013; Frey et al., 2014; Brinkerhoff et al., 2016; Rabatel et al., 2018; Maussion et al., 2019; Werder et al., 2020). This is computationally efficient as compared to calculating distributed ice thickness fields, but comes with the limitation that the physics-based inversion is only conducted at specific locations. In the second approach, a simple model considering only internal shear (i.e. the shallow ice approximation, SIA) is applied to turn a modelled or observed quantity (e.g. depth-integrated ice flux, surface velocities) into ice thickness, sometimes complemented with a parameterization for basal sliding (Farinotti et al., 2009; Huss and Farinotti, 2012; Li et al., 2012; Linsbauer et al., 2012; Paul and Linsbauer, 2012; Clarke et al., 2013; Frey et al., 2014; Gantayat et al., 2014; Fürst et al., 2017; Rabatel et al., 2018; Langhammer et al., 2019; Maussion et al., 2019; Werder et al., 2020; Zorzut et al., 2020; Millan et al., 2022). These approaches are also computationally cheap compared to calculations based on a higher-order or Full-Stokes model, and they exploit the simple mathematical nature of the depth-integrated SIA. However, the simplifying assumptions on ice dynamics that are at the heart of the SIA translate into errors in the calculated ice thicknesses at locations where the conditions are not met. Although different in their complexity, their required inputs and their strengths and limitations (for more details the reader is referred to the respective publications), the thickness inversion approaches discussed here share limitations that arise from following one or both of the mentioned strategies. For instance, using a bed derived with such methods for prognostic simulations with map-plane higher-order or Full-Stokes models requires initial model relaxation that likely results in a glacier state significantly different from observations.

A different approach was presented by van Pelt et al. (2013), building on previous work in the context of inversion problems in fluid mechanics (Heining, 2011). Using historical observations of external forcing, and starting from an initial guess for bed topography, they use the ice flow model PISM (Bueler and Brown, 2009) to simulate centuries of glacier evolution up until present day, when a comparison between modelled and observed surface elevation is made. Based on the assumption that any deviations between the two are due to errors in the bed, this mismatch is then used to update the subglacial topography. These

https://doi.org/10.5194/tc-2023-43
Preprint. Discussion started: 4 April 2023

two steps are repeated iteratively until a certain stopping criterion is reached. This approach allows to include any physics that state-of-the-art ice flow models feature and it results in a distributed map of bed topography that is in balance with the present-day dynamic state of the glacier and the external forcing. For ensuing prognostic simulations, no relaxation is needed as all input parameters and physics used for the forward simulations can also be used in the thickness inversion.

The approach by van Pelt et al. (2013) is based on the idea that the present-day dynamic state of a glacier is best reproduced by simulating that glacier for centuries up until today using historical forcing. However, such forcing data is rarely available and subject to considerable uncertainties. Furthermore, due to the long time spans modelled the approach is computationally costly. Here, we exploit the fact that the instantaneous rate of surface elevation change dh/dt, which also represents the dynamic state of a glacier, is much faster to model allowing one to apply a similar methodology as in van Pelt et al. (2013) while only requiring a fraction of the computational resources. In our new approach, we furthermore extend the capabilities of the thickness inversion in that we simultaneously infer basal friction using observed surface velocities akin to a previously published approach (Pollard and DeConto, 2012). Ultimately, we establish a framework that is able to provide a comprehensive view of the state of a glacier consistent with its external forcing, its ice dynamics and its bed topography while being at low computational cost. Allowing to choose between different levels of complexity for the ice-flow physics and whether or not to simultaneously infer basal friction, our approach is suitable both for detailed inversions at the local scale as well as for fast large-scale applications.

In the following, we describe our new fast ice thickness inversion approach using PISM as a forward model, we demonstrate its capabilities with an example of an artificial ice cap grown inside a numerical model, and apply and test it on the tidewater glacier Kronebreen on Svalbard.

2 A new thickness inversion approach

2.1 Method

The general functional principle derives from the idea that a numerical model of a glacier initialized with the correct boundary conditions should behave similarly to a real glacier; if not, one needs to conclude that the model setup is erroneous in some part. In a simple case without basal sliding and neglecting thermodynamic processes, the first-order controls on ice dynamics are the climatic mass balance, the glacier surface shape and the bed. By assuming that it is possible to set up a numerical ice-flow model where all of these inputs are sufficiently well represented except for bed topography (because they are surface observations), we may attribute any differences in modelled vs. observed ice geometry and dynamics to originate from errors in the bed.

To turn this framework into an inversion approach, the following workflow is applied (Fig. 1): First, a numerical representation of a glacier is set up inside an ice flow model with observations of surface shape from a digital elevation model (DEM) and climatic mass balance. Furthermore, some arbitrary bed shape is assumed. For instance, it is straightforward to derive a rough bed estimate from a DEM with the perfect-plasticity method (Nye, 1952; Haeberli and Hoelzle, 1995). As Habermann et al.

https://doi.org/10.5194/tc-2023-43
Preprint. Discussion started: 4 April 2023

The Cryosphere Discussions
Open Access
EGU

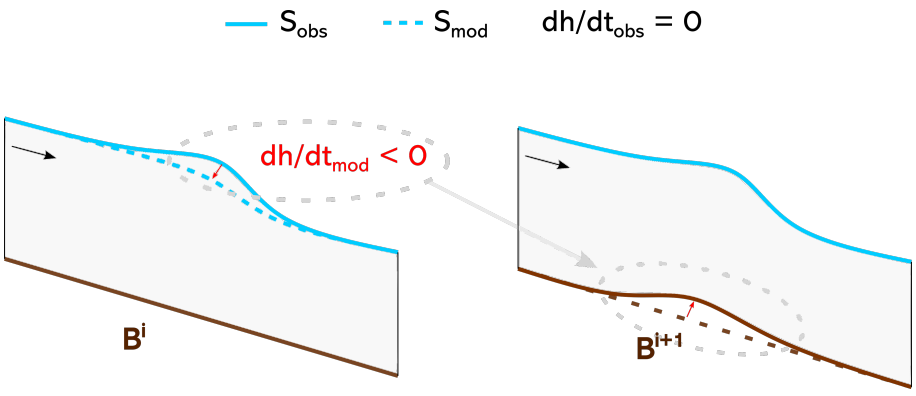

Figure 1. Schematic representation of bed corrections during thickness inversion workflow, assuming a steady-state glacier (dh/dt_{obs} = 0) with observed surface S_{obs}. Without the bed bump at iteration i, the modelled surface S_{mod} subsides during a short forward simulation, rendering dh/dt_{mod} negative. As given by eq. (1), this negative misfit between modelled and observed dh/dt results in an uplift of the bed.

(2012) points out, though, an initial bed guess should not contain roughness not justified by the input data, so some smoothing, e.g., with a gaussian filter, may be in order.

Then, the ice-flow model is run forward with the goal of comparing whether modelled and observed ice dynamics agree. As described before, the target variable here is the rate of surface elevation change dh/dt as a measure for the dynamic state of the glacier. From the model side, this requires only a stress balance simulation or a simulation with a short timescale length dt to compute the instantaneous dh/dt_{mod}. From the observational side, it requires either an already existing dh/dt product (e.g. Hugonnet et al., 2021), or two DEMs from different years, where it is assumed that the rate of surface elevation change between them is constant, allowing the derivation of the quantity dh/dt_{obs}. If $dh/dt_{mod} = dh/dt_{obs}$, it is reasonable to conclude that the bed topography is correct, because the model correctly reproduces the observations. However, in the more likely event that they are not equal, the differences between the two are ascribed to originate from errors in the bed, following the logic discussed above.

If there is a mismatch between a modelled and observed quantity, previous work has shown point-wise updates can be applied to the unknown parameter (in this case bed topography) as a simple function of that mismatch (van Pelt et al., 2013; Michel et al., 2013; Heining, 2011; Pollard and DeConto, 2012). Here, a new bed B^{i+1} is hence produced by subtracting, at any point in space in the domain, the misfit in modelled vs. observed dh/dt at that point from the present bed B^i such that

$$B^{i+1} = B^i - \beta \left(\frac{dh^i_{\text{mod}}}{dt} - \frac{dh_{\text{obs}}}{dt} \right) \tag{1}$$

where β is a scalar that controls the magnitude of bed corrections. These simple steps described here (running the model forward, computing the misfit in modelled vs. observed dh/dt and updating the bed) are repeated iteratively until a satisfactory solution for the bed is found (Fig 1). Note that van Pelt et al. (2013) used a similar equation, although instead of dh/dt,

https://doi.org/10.5194/tc-2023-43
Preprint. Discussion started: 4 April 2023

The Cryosphere Discussions

the modelled surface elevation S_{mod} after century-long time-dependent runs was used to calculate a misfit with the observed surface S_{obs}, requiring much greater computational resources.

Our experiments show that this simple approach alone is capable of recovering subglacial topography for a non-sliding glacier yielding an overall good match with the true bed. However, previous research has shown that ice thickness inversion is non-unique. Small scale bed undulations leave no expressions on the glacier surface and hence an inversion, regardless of the method used, can make no statement on the existence or non-existence of such features (Gudmundsson, 2003; Bahr et al., 2014). For our approach, this implies that the derived bed may contain such small-scale undulations that are not justified by the input data if the solution is not biased towards outcomes that take these limitations into account. Furthermore, real-world problems imply that input data and model physics are never perfect, meaning that not all deviations between modelled and observed dynamics can be attributed to originate from errors in the bed.

Previous work in the spirit of traditional inversion theory has tackled this issue by introducing so-called regularization terms which force the modelled bed to be smooth and which account for a degree of imperfection in the model (Habermann et al., 2012). Here, we present a novel way of handling this issue: every time the bed topography is updated, a small proportion θ of the dh/dt misfit is used to also update the glacier surface S in the opposite direction of the bed such that a new surface S^{i+1} is given by

$$S^{i+1} = S^i + \theta\beta\left(\frac{dh^i_{\text{mod}}}{dt} - \frac{dh_{\text{obs}}}{dt}\right). \tag{2}$$

Doing so results in a 'squeezing' effect where an upwards correction of the bed (i.e. the ice thickness becomes smaller) results in a lowered glacier surface at that point, and vice versa for a downwards bed correction. This leads to locally steeper surface slopes and therefore increased driving stresses which gently induce further bed corrections in surrounding areas, thus evening out small bed undulations. At the same time, the small changes in the surface shape allow the model to accommodate observations which it otherwise cannot reproduce, be it because of input errors or imperfect model physics. Indeed, our experiments show that the bed and surface updates interact to finally yield a configuration where $dh/dt_{mod} = dh/dt_{obs}$.

Finally, our method works well under the assumption that sliding is not significant. Where this simplification does not hold, one solution is to prescribe some friction field. However, this makes the modelled ice thickness dependent on an often poorly constrained parameter which could lead to considerable errors in the recovered bed. Here, we address this issue by inverting for basal friction following a similar methodology as in Pollard and DeConto (2012). Most sliding laws have a parameter (often termed friction coefficient, yield stress, etc.) that varies in space but is constant in time which controls the strength of the subglacial material, and hence the amount of sliding. We invert for this parameter F in a similar fashion as shown before. Specifically, again an initial guess for F is made which is subsequently updated, however, this time using a mismatch in modelled vs. observed ice flow speed u, such that

$$F^{i+1} = \begin{cases} F^i - \lambda F^i, \text{ if } \frac{u^i_{\text{mod}} - u_{\text{obs}}}{u_{\text{obs}}} < -\lambda \\ F^i + \lambda F^i, \text{ if } \frac{u^i_{\text{mod}} - u_{obs}}{u_{\text{obs}}} > \lambda \\ F^i + F^i\left(\frac{u^i_{\text{mod}} - u_{\text{obs}}}{u_{\text{obs}}}\right), \text{ otherwise.} \end{cases} \tag{3}$$

https://doi.org/10.5194/tc-2023-43
Preprint. Discussion started: 4 April 2023


The Cryosphere Discussions
Open Access
EGU

The parameter λ serves to prevent too strong updates to the friction field. Importantly, bed and friction are not updated in the same iteration. This is because the dh/dt misfit and the velocity misfit both represent a mismatch in modelled vs. observed flow dynamics and it is not clear how to disentangle which part of that mismatch is due to an erroneous friction field vs. an erroneous bed. So instead, F is only updated once after the model has converged to a solution for ice thickness. At that point, a model configuration that can explain dh/dt_{obs} has been found. However, only if that model also explains observed surface speed is it reasonable to conclude that the imposed friction field is correct, assuming that the friction field is the largest remaining unknown control on ice dynamics. If there is no agreement in modelled vs. observed surface speed, F is likely not correct (again under that same assumption) and hence the modelled bed elevation is erroneous. A change in the friction field will trigger a response of the ice dynamics, and so dh/dt_{mod} will no longer match dh/dt_{obs} after having updated F. Following a friction update, a new bed thus needs to be found that can explain dh/dt_{obs} with that new friction field. Therefore, again bed and surface updates according to eq. (1) and (2) need to be applied until any dh/dt mismatch is resolved. Subsequently, the velocity mismatch is evaluated and if needed, F is updated. Ultimately, this alternation between many bed updates and one friction update is repeated until a combination of a bed and friction field is found that explains both dh/dt_{obs} and u_{obs}.

2.2 Model

While the method is not bound to a specific ice-flow model, we use the Parallel Ice Sheet Model (PISM v.2.0.4, Bueler and Brown (2009)) for the ice-flow simulations. Below, we briefly present relevant aspects of PISM with respect to our thickness inversion method, but refer the reader to the literature for a more in-depth description (Bueler and Brown, 2009; Winkelmann et al., 2011).

PISM allows the glaciological stress-balance equations to be solved using one of four approximations to the Full-Stokes equations: the shallow ice approximation (SIA), the shallow shelf approximation (SSA), a hybrid SSA+SIA scheme or the Blatter-Pattyn higher-order model (Blatter, 1995; Pattyn, 2003). Any of them is suitable for the thickness inversion, but we here apply the hybrid SSA+SIA scheme. To simulate sliding, different laws are available, some of which allow interaction with modelled thermodynamics to yield values of subglacial water availability which in turn determines basal friction. In this work, we do not include thermodynamic processes (sec. Discussion), and rely instead on a simple pseudo-plastic power law where basal shear stress $\boldsymbol{\tau}_b$ is given by

$$\boldsymbol{\tau}_b = -\tau_c \frac{\boldsymbol{u}}{u_{th}^q |\boldsymbol{u}|^{1-q}} \tag{4}$$

where u_{th} is the threshold velocity where τ_b has the same magnitude as the yield stress τ_c and $q \in [0,1]$ is an exponent determining the plasticity of the sliding law ($q = 1$ represents a linear sliding law). τ_c is a spatially variable constant which reflects the strength of the subglacial bed and hence determines the degree of sliding. This is the quantity that we invert for in eq. (3).

https://doi.org/10.5194/tc-2023-43
Preprint. Discussion started: 4 April 2023

The Cryosphere Discussions

Table 1. Parameter values used for building the ice cap and the subsequent inversion.

Parameter	Value
Ice temperature	268 K
Ice density	910 $kg\ m^{-3}$
q	0.333
u_{th}	1 $m\ s^{-1}$
β	1
θ	0.025
dt	0.1 yr
λ	0.5

3 Synthetic experiments

3.1 The synthetic ice cap

We start by using our new method on an artificial ice cap. We first design a domain with a 50 x 50 grid and a resolution of 2 km where we define a bed topography consisting of a flat bed including two large (500 m tall) and two small (350 m tall) bumps with a prescribed mass balance field (Fig. 2a). Furthermore, we design a friction field by setting the parameter τ_c such that the left half of the domain is slippery, allowing ice to slide, while the right half is sticky, preventing any basal motion. We use a non-linear sliding law as in the MISMIP experiments (Pattyn et al., 2012) by setting the sliding law parameters $q = 1/3$ and $u_{th} = 1m\ s^{-1}$ in eq. (4) (Tab. 1). Subsequently, we grow the ice cap inside PISM for 10 kyrs using the isothermal SSA+SIA scheme allowing us to obtain a steady-state configuration with a maximum ice thickness of ∼1000 m. Then, we 'forget' the bed and friction field and try to recover them. For the thickness inversion, we use as inputs the same mass balance as applied when growing the ice cap, the surface of the grown ice cap, a reference dh/dt_{obs} field that is zero everywhere (since the ice cap is in steady-state), and make a first bed guess assuming a completely flat bed without bumps (Fig. 2a). For the friction inversion, our first guess is that the domain is sticky everywhere, and the input required to later update this guess is the velocity field of the grown ice cap. Subsequently, we simulate a short forward run with $dt = 0.1$ yrs and update the bed and the ice cap surface according to eq. (1) and (2). To prevent irregularities at the ice cap margins where spurious boundary effects can occur, we do not apply any updates in a band of two cells width at the ice cap margin, but set the bed elevation to zero there. As we iteratively update the bed and the surface in that way, we calculate for all n grid points inside the ice-covered domain the median dh/dt misfit Δdh defined as

$$\Delta dh = med\left(\frac{dh_{mod}}{dt} - \frac{dh_{obs}}{dt}\right), \tag{5}$$

and the mean absolute bed misfit $\overline{|\Delta B|}$, given by

https://doi.org/10.5194/tc-2023-43
Preprint. Discussion started: 4 April 2023

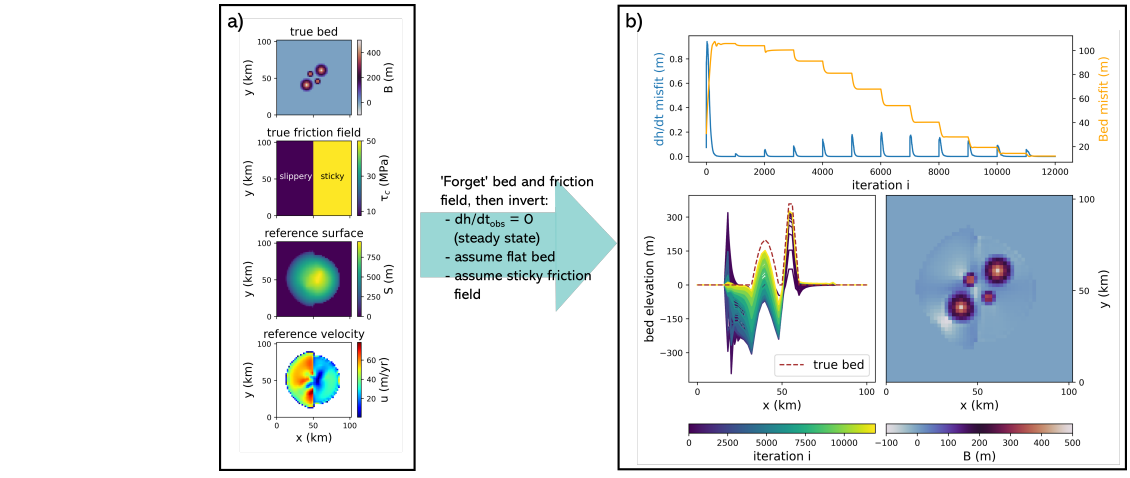

Figure 2. Example of the thickness inversion for a 'home-grown' ice cap (i.e. ice cap is created, then the bed and friction field is 'forgotten' before the inversion is run with the same physics as the build-up). a) Bed and friction field used to build the ice cap plus the surface elevation and velocity of the artificial ice cap. b) dh/dt and bed misfit per iteration step i with sharp peaks and distinct steps indicating times at which friction field was updated (top panel). Cross-section through bed along y=23 km at each iteration step (lower left) and final bed elevation after 12000 iterations (lower right panel)

$$\overline{|\Delta B|} = \frac{1}{n}\sum_{1}^{n}|B_{mod} - B_{ref}|. \tag{6}$$

After 1000 iterations, we apply a friction update according to eq. (3). Note that this amount of iterations between friction updates is rather arbitrary; we here choose it simply because this number is large enough to ensure that the dh/dt misfit is sufficiently small at that point so that no more bed updates are occurring. While $\overline{|\Delta B|}$ is generally reduced as the iterative inversion progresses, each friction update induces a short response in the ice dynamics that briefly increases the Δdh.As seen in Fig. 2b, the steep decline of the bed misfit at these instances highlights that those friction updates are crucial for finding the correct bed. Indeed, a cross-section through the icecap reveals that the bed in the right (sticky) half of the domain is correctly identified already before the first friction update. In the left (slippery) half where the initial friction field does not allow any sliding, however, ice thickness is greatly overestimated at that point. This is because in the absence of sliding, the ice thickness needs to be much greater to be able to achieve an ice flux that is in line with dh/dt_{obs} and mass balance. With each friction update, the bed is made more slippery which increases flow velocities, thins the ice and lifts up the bed until eventually the correct bed is found here as well. The final bed is in good agreement with the original one (Fig. 2).

https://doi.org/10.5194/tc-2023-43
Preprint. Discussion started: 4 April 2023

3.2 Ice cap sensitivity

Next, we explore how sensitive the inversion is to errors in the input data and to modelling choices. To that end, we use the synthetic ice cap where we have full knowledge of the 'true' parameters. In the following, we provide an overview of the results, while detailed figures and more elaborations can be found in the appendix.

3.2.1 Input errors

We test the sensitivity to changes in the input mass balance (which is equal to modifying dh/dt, since it can be shown that those two parameters may be understood as one through the concept of the *apparent mass balance* (Farinotti et al., 2009)) and velocity in experiments where their magnitude is reduced or increased by 25%, 50% and 75%, respectively, relative to their true value. Furthermore, we conduct experiments where we introduce random surface elevation noise with a standard deviation of 5 m, 10 m, 15 m, 25 m and 50 m. Finally, we modify the ice temperature from its true value of 268 K to values of 264 K, 266 K, 270 K and 272 K. For the sensitivity tests of mass balance and ice temperature, we investigate two scenarios: in one, we assume that the true friction field is known, and hence no friction updates are applied; in the other, we assume no prior knowledge of the friction field, requiring inversion for this parameter.

With a known friction field, mass balance errors translate to ice volume errors as the 5th root, as is expected from theory for shear-dominated flow (Cuffey and Paterson, 2010). With friction updates, however, mass balance (and dh/dt) errors are reinforced. Consider, for instance, a negative mass balance error: this yields overall smaller ice thicknesses and therefore reduced driving stresses, which in turn results in slower ice flow. To match the observed velocities, sliding must be increased when friction updates (eq.(3)) are applied, resulting in further thinning of the ice. The same effect but with opposite sign follows from a positive mass balance errors.

Errors in the observed ice velocity induce similar mechanisms. A negative error here means that the bed is made more sticky than it should be, resulting in too thick ice. However, this overestimation of ice thickness induces too-large ice-deformational velocities, leading to an even more sticky bed when eq. (3) is applied, thus causing further thickening. Again, the opposite is the case for a positive velocity error.

In the case of ice temperature errors, friction updates have a compensating effect. For instance, a negative ice temperature error causes too-stiff ice and hence too-slow flow, which leads to too-thick ice without friction updates. With friction updates, however, too-slow flow results in a negative velocity mismatch (eq. (3)) leading to a more slippery bed which, in turn, thins the ice again. Overall, the exact magnitude of amplifying or damping effects of friction updates in the presence of errors in ice temperature, mass balance, dh/dt and velocity depends on several characteristics that vary between glaciers, e.g. sliding magnitude and extent, and is thus hard to generalize.

For surface noise, we find that it changes the bed shape, with already small surface perturbations causing large bed responses, as is expected from theory (Raymond and Gudmundsson, 2005; Bahr et al., 2014). However, increasing the regularization parameter θ serves to mitigate these issues, although it makes the final bed shape more dependent on initial conditions. Furthermore, we find that the calculated final ice volume is largely insensitive to surface noise.

https://doi.org/10.5194/tc-2023-43
Preprint. Discussion started: 4 April 2023

3.2.2 Inversion parameters

We now investigate how different parameter choices for the inversion influence results. Specifically, we investigate the length dt of the ice-flow model forward simulation, the relaxation parameter β (eq. (1)), the regularization parameter θ (eq. (2)) and the role of initial conditions.

We find that our results show virtually no dependence on dt. Likewise, the recovered bed and friction field is not sensitive to their initial guess. For β, larger values lead to faster convergence, but lower detail in the recovered bed as compared to smaller values. This is because a large β can cause the bed to oscillate around its true value. The largest influence on the recovered bed is θ which serves to balance observations and model physics in the presence of input errors as well as to regularize the solution. Larger expected errors in input data require larger θ to allow the model to accommodate these 'unreproducible' characteristics of the data. As mentioned previously, however, this increases the dependence on initial conditions since it means that also parts of the non-erroneous observations are accommodated by surface updates rather than bed adjustments. Regardless of the quality of the input, we find that choosing $\theta > 0$ is beneficial to avoid small bed irregularities in the solution which are not justified by the input data.

4 Application to Kronebreen

Next, we apply our method to the tidewater glacier Kronebreen on Svalbard. With Kronebreen we here refer to a combined glacier system consisting of the ice cap Holtedahlfonna, feeding the outlet glacier Kronebreen. The glacier system covers an area of $\sim$380 km^2 and an elevation range from sea level to around 1400 m. Highest flow velocities of up to $>$1000 m a^{-1} are found on the highly crevassed glacier tongue (Schellenberger et al., 2015). Due to the large availability of in situ and remote sensing data, Kronebreen has in recent years been subject of numerous glaciological studies on ice dynamics (e.g. Schellenberger et al., 2015; Vallot et al., 2017), mass balance (e.g. van Pelt and Kohler, 2015; Deschamps-Berger et al., 2019), subglacial hydrology (How et al., 2017), calving (Luckman et al., 2015; Vallot et al., 2018), perennial firn aquifers (Christianson et al., 2015), seismicity (Köhler et al., 2019) and basal topography (Lindbäck et al., 2018).

4.1 Observational data

The input data for the thickness inversion of Kronebreen comprises two DEMs based on Pleiades imagery from 2014 (Deschamps-Berger et al., 2019) and 2020 which we use to generate a dh/dt field $\frac{dh}{dt}_{obs} = \frac{S_{2020} - S_{2014}}{6}$ (Fig. 3). The 2020 DEM has some holes at higher elevations in the southern part of Kronebreen which we fill using 2014 data. Since dh/dt hence would be zero there, we generate a dh/dt field as a function of surface elevation which we use to patch those holes. Whether to use the 2014 DEM, the 2020 DEM or a mean of the two as input surface for the ice dynamics model is not an obvious choice. From a theoretical point, the surface that gave rise to (or was the product of) the aggregate ice dynamics in the period 2014-2020 should be used. While this would favor using the mean of the two DEMs, it would imply using a surface that may not have existed ever. We therefore choose to use the 2020 DEM instead as this avoids complications at the terminus where Kronebreen has

https://doi.org/10.5194/tc-2023-43
Preprint. Discussion started: 4 April 2023

retreated. There, differencing or taking a mean of the two DEMs would not yield a representative dh/dt field or glacier surface because the difference and mean between the 2014 surface elevation and sea level (which is what the 2020 DEM shows) does not reflect the true ice loss or a realistic glacier surface shape. We also smooth the input DEM with a gaussian kernel prior to feeding it to the inversion algorithm. In terms of mass balance, we use observations from ten stakes placed approximately along the central flow line of Kronebreen and covering an altitude range from 505 m (mean over 2014-2020: -0.53 m w. eq. yr^{-1}) to 1116 m (mean: 0.96 m w. eq. yr^{-1}) to generate a linear mass balance gradient which we apply over the whole altitudinal range of Kronebreen. Following general observations made at glaciers in Svalbard, we cap the maximum mass balance at 1 m yr^{-1} (similar to van Pelt and Kohler (2015)). Internal and basal mass balance are neglected. Finally, we use surface velocity observations from Millan et al. (2022) with a nominal date 2017-2018. Their performance is validated using measured stake velocities (mean difference: 2.4 m yr^{-1} / 3.5%).

For validation of the modelled thicknesses, we use an extensive data set of measured bed elevations acquired using ground-penetrating radar (Lindbäck et al., 2018). The errors associated with that data are on the order of 10 m where the ice is thin (mainly along the fast-flowing lower reaches of Kronebreen) and up to 30 m in the upper thick parts of Kronebreen. We resample the radar tracks to a grid of 400 m resolution to match it with the model results.

4.2 Modelling choices

We set up a rectangular modelling domain with a regular grid spacing of 400 m. We define a glacier mask based on manually drawn outlines of Kronebreen using satellite imagery and ice flow observations. Inside the mask, we allow ice to exist while in all other parts of the domain, the ice thickness is forced to zero by removing any ice existing there after each iteration. The mask also covers some small parts of what is believed to belong to the neighboring glacier Kongsbreen where we have a surface DEM from 2020. Since the boundary between Kronebreen and Kongsbreen is not perfectly known, some ice exchange here cannot be excluded. While our experiments indicate that this is a better approach than cutting the mask at the assumed Kronebreen/Kongsbreen border (not shown), some boundary effects can still not be ruled out since we only model a small part of Kongsbreen, thus not accounting for the entire mass flux potentially reaching the Kronebreen/Kongsbreen border in reality. At all other mask boundaries, we do not apply any flux constraints or lateral friction since the friction inversion will account for lateral drag if needed.

At the glacier terminus, we apply the hydrostatic water pressure. We also remove all floating ice and do not allow calving; this is because we cut off all ice outside the mask after each iteration anyway, hence artificially 'calving' all ice that has advanced beyond the known glacier extent. Furthermore, it needs to be ensured that in each forward simulation, the ice can advance into the ocean unblocked by the bathymetry in front of the glacier (which is unknown). We therefore apply a zero bed-slope in the flow direction at the ice-ocean boundary.

Ice flow is described by the SSA+SIA hybrid scheme available in PISM (Bueler and Brown, 2009). Note that while the SSA accounts for membrane stresses, the SIA does not and so ice flows strictly downhill in the absence of sliding (see sec. 4.5). Furthermore, we set an isothermal flow law with a fixed ice temperature of 0°C where the ice softness $A = 3.96 \times 10^{-24}$ s^{-1} Pa^{-3}. While this ice temperature assumption is a simplification not valid everywhere, it follows from observations and modelling at

https://doi.org/10.5194/tc-2023-43
Preprint. Discussion started: 4 April 2023

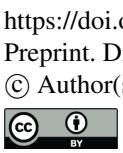

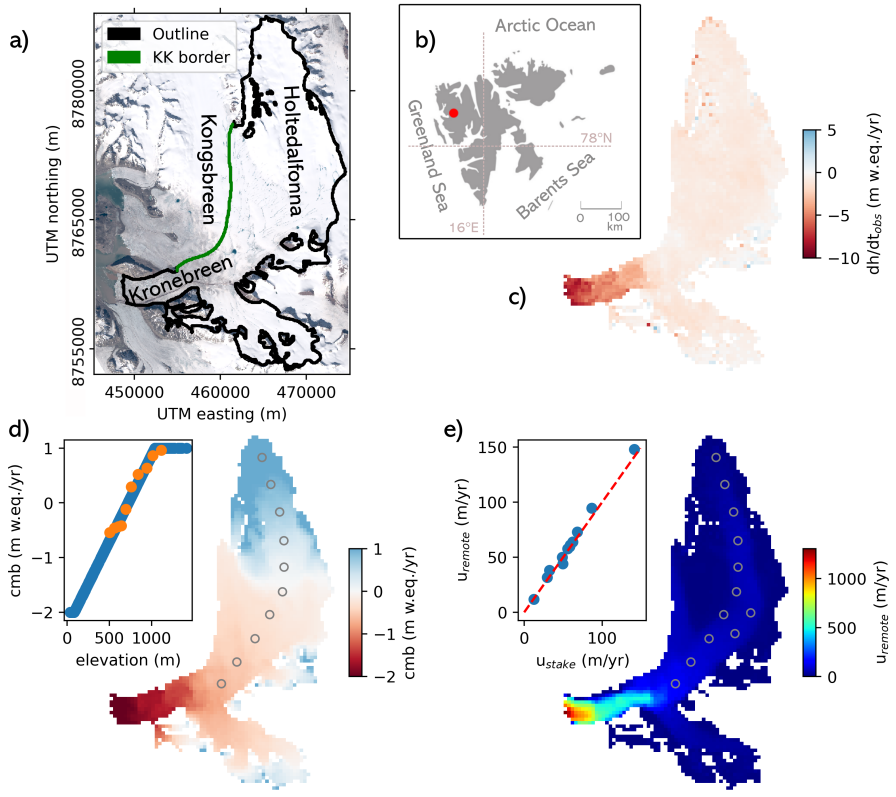

Figure 3. Input data for Kronebreen inversion (coordinate system is UTM zone 33N). a) Kronebreen outline in black and border to neighboring glacier Kongsbreen (KK border) in green; b) Location of Kronebreen in Svalbard (marked by red dot); c) observed rate of surface elevation change dh/dt as computed by subtracting two digital elevation models; d) climatic mass balance derived from extrapolating stake observations (locations shown by circles in main plot, and values by orange dots in inset) to the entire glacier using an elevation dependent linear model (inset plot); e) observed velocities from remote sensing (Millan et al., 2022) validated with stake observations (inset plot)

many Svalbard glaciers where extensive meltwater refreezing in the firn keeps the ice close to the melting point (e.g. van Pelt et al., 2019). In the bare ice areas of the ablation zone and near the glacier edges, the largest deviations from this assumption can be expected. We choose a linear sliding law by setting the parameters $q = 1$ and $u_{th} = 1\ ms^{-1}$ in eq. (4). This causes the sliding velocity to be directly proportional to the velocity misfit (eq. (3)), thus stabilizing the inversion.

4.3 Initial conditions

We derive an initial bed guess by subtracting, from the input 2020 DEM, an initial ice thickness H_{init} calculated with the perfect plasticity assumption (Nye, 1952), such that

$$H_{init} = \frac{\tau_b}{\rho g \sin\alpha}, \tag{7}$$

https://doi.org/10.5194/tc-2023-43
Preprint. Discussion started: 4 April 2023

where ρ is the ice density, g is gravitational acceleration, α is surface slope as computed from the input DEM and τ_b is the basal shear stress which we arbitrarily set to $\tau_b = 120$ kPa. Based on the sensitivity experiments with the artificial ice cap, we do not expect the choice of τ_b to impact our results significantly. We iteratively smooth the derived thickness field over four times the ice thickness to account for longitudinal stress gradients (Kamb and Echelmeyer, 1986), and we apply a gaussian kernel to remove small-scale variability not justified by the input data (Habermann et al., 2012).

For basal friction, we derive an initial guess of τ_c in eq. (4) as $\tau_c = \frac{\tau_d u_{th}}{u_{obs}}$ where τ_d is the driving stress at the start of the inversion calculated as $\tau_d = \rho g H_{init} \tan\alpha$ (Vallot et al., 2017).

4.4 Inversion parameters

We set the forward-modelling time step $dt = 0.01$ yrs. This small value allows a fast inversion while our experiments show that the results are not sensitive to this choice. For the scaling parameter β (eq. (1)), we apply a 'ramp-up' procedure where we let β increase as a function of the iteration count c, such that $\beta = \frac{-10 \cdot \beta_0}{c+10} + \beta_0$, where $\beta_0 = 0.5$. After each friction update, c is reset to one. We do this since we know that the dh/dt misfit, and hence the bed corrections, are generally largest at the start of the inversion and after friction updates; to stabilize the inversion, we find that it is beneficial to scale the bed updates with a small β at those points. Since we assume that we have high-quality input data, we apply only weak regularization by setting the parameter $\theta = 0.05$, meaning that 5% of bed updates are changing the surface in the opposite direction. Based on our experiments, we see that after ∼8000 iterations, no more changes to bed or friction field occur, and so we stop the inversion there. We also see that it takes at most ∼1000 iterations after a friction update to converge to a solution, making this our interval for updates of τ_c (eq. (3)).

4.5 Inversion results

We find that the iterations consistently reduce the dh/dt misfit (eq. (1)), interrupted by friction updates, as expected (Fig. 4a). Owing to the surface updates, the misfit approaches zero in each interval between friction updates, showing that with our regularization method, no stopping criterion is needed. It turns out that our initial bed guess overestimated ice thickness in most parts of the domain as the bed generally becomes shallower. This is particularly true at the fast-flowing outlet glacier where the friction updates decrease basal drag and thus are instrumental in ensuring that ice thickness there is not overestimated. The final mismatch between modelled and observed velocity magnitudes is generally on the order of a few percent where the glacier is sliding, while they can be higher in the non-sliding parts of the accumulation area (Fig. 4b). Overall, this indicates that the friction updates have helped to align model dynamics with reality.

When comparing with observed bed elevations from radar measurements, we see that our ice thickness generally matches the observations well with deviations on the order of a few 10s of meters (Fig. 4). However, there is one larger area where our ice thickness is greatly overestimated by more than 250 m (Fig. 4c). This area is a flat and slow-flowing part which, as shown by the observed flow-velocities, is only weakly connected to the main flow and hence only receives little ice from upstream (Fig. 4d). However, in our model, we see that there is a distinct 'flow channel' diverging from the main flow through which ice is discharged into that area. Where the 'flow channel' diverges in the model, basal velocities are close to zero, meaning that

https://doi.org/10.5194/tc-2023-43
Preprint. Discussion started: 4 April 2023

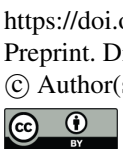

The Cryosphere
Discussions
Open Access
EGU

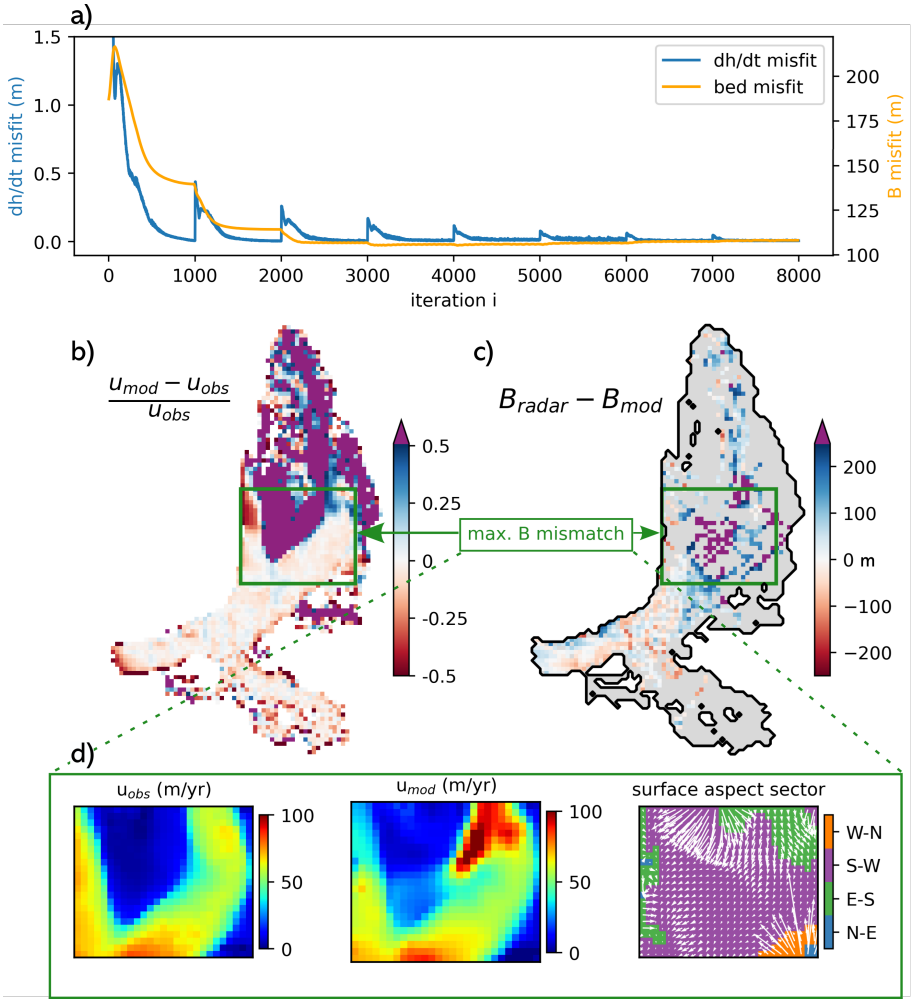

Figure 4. Raw output of Kronebreen inversion. a) dh/dt (eq. (1)) and bed misfit (eq. (6)) per iteration. b) Velocity misfit with purple color indicating where modelled velocities exceed observed velocities by more than 50%. c) Difference between radar-derived and modelled bed elevation. d) Zoom into area with largest bed deviations (green box in middle row) for observed velocities, modelled velocities and surface aspect (with arrows denoting downhill direction, and colors showing into which sector the ice surface is sloping)

internal shear controls ice flux. As mentioned before, in the absence of sliding, the shear-dominated flow calculated by the SIA is strictly downhill. And indeed, we see that our input DEM is sloping towards the 'flow channel' in that area (Fig. 4d). We hence conclude that in reality, there are likely membrane stresses forcing the ice to not flow downhill which are not resolved by our model physics, thus causing a mismatch in flow directions. Because of that, our model discharges ice into a slow and flat area where, as is known from theory (Gudmundsson, 2003; Raymond and Gudmundsson, 2005), errors in the flux will lead to large errors in the bed. Note that friction updates are of no help here: since the ice is too thick in the area, ice velocities in the

https://doi.org/10.5194/tc-2023-43
Preprint. Discussion started: 4 April 2023

model are larger than in reality due to enhanced internal deformation, which means that a friction update makes the bed more sticky (even if there already is no sliding) - while the opposite would be needed to lift up the bed.

This being said, we can still use the velocity observations to identify areas that are likely too thick. We do so by scanning our model domain for areas where the ice velocity through internal deformation exceeds the observed velocities. Assuming that our ice viscosity estimate is correct, a too-large ice thickness is the only first-order control on ice dynamics not constrained by the inputs that could induce higher velocities than observed in the absence of basal sliding. We apply this logic and conservatively only mark areas where the observed ice velocity is exceeded by at least 50% to account for errors in the velocity observations (purple areas in Fig. 4b). And indeed, this reliably identifies the area where the mismatch in flow directions induces the largest errors in the modelled bed, as well as picking out other locations where the ice thickness is overestimated (as shown by the radar validation). To update the bed elevation estimate in this area, we turn towards an analytical ice thickness equation based on the SIA (e.g. Millan et al., 2022) in which ice thickness H can be inferred from observed velocities such that

$$H = \left(\frac{(u_{s+} - u_b)(n+1)}{2A(\rho g \alpha)^n} \right)^{\frac{1}{n+1}} \tag{8}$$

with $n = 3$ being Glen´s flow law exponent (Glen, 1955) and u_s and u_b surface and basal velocity, respectively. Note that this equation requires a minimum slope α_{min} which we set to 0.025 (e.g. van Pelt et al., 2013) to prevent ice thickness going to infinity as α approaches zero. Furthermore, note that u_{s+} here refers to $u_s + 0.5u_s$ to account for the uncertainty in velocities. With this post-processing step, we are able to greatly reduce the errors in the modelled bed. Where we have identified and corrected the bed based on the mismatch between ice-deformational and observed velocities, errors have decreased by several hundreds of meters. We derive a final bed product by smoothing the computed bed with a gaussian kernel and so arrive at a mean absolute deviation from observations (eq. (6)) of 78 m (as compared to 108 m for the raw output prior to post-processing) (Fig. 5).

From our input datasets, the least constrained one is arguably surface mass balance, since we rely on a few stakes that are extrapolated to the entire glacier. An ice core drilled in 2005 on an ice divide in the upper accumulation area (1200 m a.s.l.) of Kronebreen indeed shows considerably lower accumulation (0.5 m w.e. yr^{-1} during 1963-2005, (van der Wel et al., 2011)) than the values we use here (1 m w.e. yr^{-1}), demonstrating that there is large spatial inhomogeneity, likely as a result of variability in wind exposure and associated snow redistribution. This is also known from other Svalbard glaciers (e.g. van Pelt et al., 2014). The velocity misfit map of our raw output indicates that in large parts in the accumulation area the ice is flowing too fast despite no or very limited basal sliding. While this could also be the result of a too-high ice viscosity (note, however, that we already use an ice temperature of 0°C), a likely explanation is a too positive mass balance which induces too thick ice and hence too fast surface motion by internal deformation. We therefore repeat our thickness inversion after multiplying the mass balance by 0.8. Indeed, this yields a better result with a mean absolute deviation of 100 m (was 108 m) before post-processing. The velocity misfit in the accumulation area is also reduced.

https://doi.org/10.5194/tc-2023-43
Preprint. Discussion started: 4 April 2023

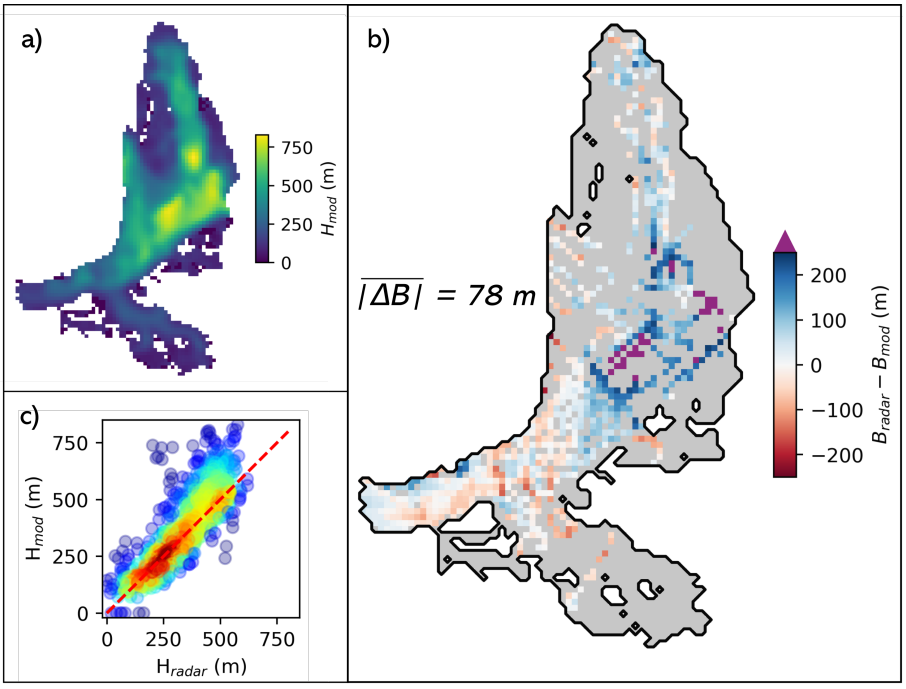

Figure 5. Final output after 'post-processing'. a) Modelled ice thickness. b) bed elevation error as compared to radar observations, with mean absolute error (eq.(6)) of 78 m. c) Correlation between radar-derived and modelled ice thickness.

5 Discussion and conclusions

We here presented a new thickness inversion method and tested it on both a synthetic ice cap as well as the tidewater glacier Kronebreen in Svalbard. The input datasets are easily-obtainable surface observations where ready-to-use products already exist on a global scale (dh/dt_{obs} by Hugonnet et al. (2021), surface velocities by e.g. Millan et al. (2022), DEMs from e.g. NASA JPL (2020), glacier outlines from RGI Consortium (2017), mass balance by Rounce et al. (2023)). Observations of bed height are not required. The key strength of the method lies in the fact that it produces distributed maps of ice thickness and basal friction using any level of complexity in ice physics, while being computationally cheap. In essence, the inversion output is not only a bed and friction map, but a fully spun-up glacier model that reproduces the present dynamic state of the modelled glacier as constrained by observations. Therefore, using the output for prognostic simulations is possible without requiring any further model relaxation.

Although always converging to a bed solution, the experiments with the synthetic ice cap showed that errors in input data can have varying impacts on the modelled bed depending on the inversion setup. With friction updates, the method is less sensitive to errors in ice temperature than without friction updates, since the modelled basal friction field can compensate for ice viscosity errors. However, the method is more sensitive to errors in mass balance and dh/dt with friction updates since an underestimation (overestimation) of mass flux and hence ice thickness reduces (increases) internal deformation, prompting

https://doi.org/10.5194/tc-2023-43
Preprint. Discussion started: 4 April 2023

changes in the friction field that further exacerbate the error. Likewise, errors in velocities reinforce themselves. Because of that, we argue that friction updates should be used with caution, i.e. only when it is likely that sliding is important for a specific glacier and when the input data is of sufficient quality. Indeed, for both the synthetic ice cap and Kronebreen, not doing friction updates would have required us to assume a friction field without any knowledge of whether it is reflective of the 'true' basal conditions or not, hence resulting in a somewhat arbitrary bed shape. For slow-flowing mountain glaciers with only poor velocity observations, however, it may be more meaningful to assume a friction field or simply not allow any sliding. In the case of non-sliding mountain glaciers with high-quality velocity data, velocity observations could be used to tune the ice temperature. Regarding errors in an input DEM, we showed that our regularization methodology involving small adjustments to the surface in each iteration is capable of producing a reasonable bed shape even in the presence of considerable surface errors, albeit with less spatial detail and stronger dependence on initial conditions for larger values of the regularization parameter θ. Generally, the comparatively large sensitivity of a bed inversion to the input surface is an inherent problem that follows from the ill-posed nature of all thickness inversions, and is thus largely unavoidable (Bahr et al., 2014). Since global DEMs are generally quite accurate though (Chen et al., 2022), we anticipate that surface elevation may be a smaller problem for regional ice thickness inversion than the available glacier outlines which sometimes include ice-free areas (RGI Consortium, 2017) that may induce unphysical results.

The inversion method presented here places great weight on internal model consistency. While this ensures that the output will be in line with all fundamental principles of ice dynamics as represented in ice flow models, it also means that a real-world process that is not reflected in the physics of the forward model will - if not accounted for otherwise - result in errors in the bed shape. As such, unregularized data and model errors are subsumed in the final bed as seen for the Kronebreen experiments. While it is possible to estimate how errors in the input data are propagated to bed errors, this is unfortunately not true for model errors which are difficult to quantify. Using our 'post-processing' approach as outlined in sec. 4.5, however, allows alleviation of some of the possible errors. Such an approach represents an interference with model physics in favor of a more accurate bed map, and should therefore be applied when the modelled bed likely contains significant errors. This may be assessed based on the mismatch in observed and modelled velocities as shown here. If only minor deviations are found, we propose to refrain from any post-processing to conserve the consistency between bed, model physics and input observations.

We do not consider thermodynamics in this study, but use a constant ice viscosity parameter. This could account for some errors that we see at Kronebreen such that, for instance, a locally stiffer ice body might have resulted in slightly different modelled flow directions in those places where we find the largest errors. How to implement thermodynamics in our inversion methodology should hence be explored in future work.

Code and data availability. PISM v.2.0.4 is freely available for download at http://www.pism.io/. Note that PISM needs to be built including PISM´s Python bindings for optimal computational performance. Key scripts needed to perform the simulations done in this study will be made publicly available on GitHub once the manuscript is published. Radar data for Kronebreen are available at https://doi.org/10.21334/npolar.2017.702ca4a7(Lindbäck et al., 2018), and ice velocity at https://doi.org/10.6096/1007 (Millan et al., 2022)

https://doi.org/10.5194/tc-2023-43
Preprint. Discussion started: 4 April 2023

Appendix A

Below, we elaborate further and present figures on the sensitivity experiments described in sec. 3.2.

A1 Input errors

We start by perturbing the mass balance such that it is reduced and increased uniformly in the domain by 25%, 50% and 75%. Mass balance and dh/dt jointly control the mass flux through the glacier (and can even be lumped together into one variable, following the concept of the apparent mass balance (Farinotti et al., 2009)), and so errors in either of them have the same effect. Therefore, we do not investigate them separately here, but focus on mass balance alone. A reduction in flux should lead to a thinner glacier and shallower bed while the opposite should be the case for an increase in flux, as observed in our experiments (Fig. A1). From the integrated form of Glen´s flow law (Cuffey and Paterson, 2010) for shear-dominated flow

$$H = \sqrt[n+2]{\frac{q}{2A} \cdot \frac{n+2}{(\rho g \sin\alpha)^n}}, \tag{A1}$$

it can be seen that flux (denoted by q) errors translate into thickness errors as the 5th root. If we prescribe the true friction field at the start of the inversion and do not apply any updates to it, the computed ice volumes using the perturbed mass balances follow this relationship accurately. However, with friction updates, there are positive feedback effects which induce larger errors. Since a reduction in mass flux means that the calculated ice thickness is smaller than its true value, the driving stresses are smaller, resulting in slower ice flow. To match the observed velocities, sliding must hence be increased when friction updates (eq. (3)) are applied, resulting in a further thinning of the ice through associated bed uplift. Therefore, with friction updates the final ice volume is smaller than what might be expected from the mass balance underestimation alone. The opposite is the case when the mass flux through the glacier is overestimated. In this case, the overestimated ice thickness induces larger driving stresses and hence an overestimation in surface velocities, prompting the friction field to be made more sticky during a friction update. This induces further bed lowering, resulting in a stronger overestimation of ice thickness at the end of the inversion. This effect, however, is only present in those areas where the glacier is sliding. In non-sliding areas, a further increase in the friction field will not lead to a thickness increase, putting an upper bound on this positive feedback effect. To quantify the effects of flux errors when friction updates are applied is, therefore, more difficult than when no friction updates are applied. Both the ratio between sliding and non-sliding areas in the glacier as well as the sliding magnitude control the final errors. Generally though, due to the above, an underestimation of ice flux introduces larger errors than an overestimation, and so we find that for our artificial ice cap, negative mass balance errors translate about linearly into volume errors, while positive ones introduce errors to a power somewhat below one (Fig. A1).

Next, we assume errors in the velocity field by increasing and reducing the reference velocities by 25%, 50% and 75% uniformly throughout our domain (Fig. A2). Generally, a positive error in 'observed' velocities should lead to a shallower bed and hence a thinner ice cap because faster 'observed' velocities mean that the bed must be more slippery under the same mass flux. However, again a positive feedback mechanism acts on top of that: a thinning of the ice leads to a reduction in driving

https://doi.org/10.5194/tc-2023-43
Preprint. Discussion started: 4 April 2023

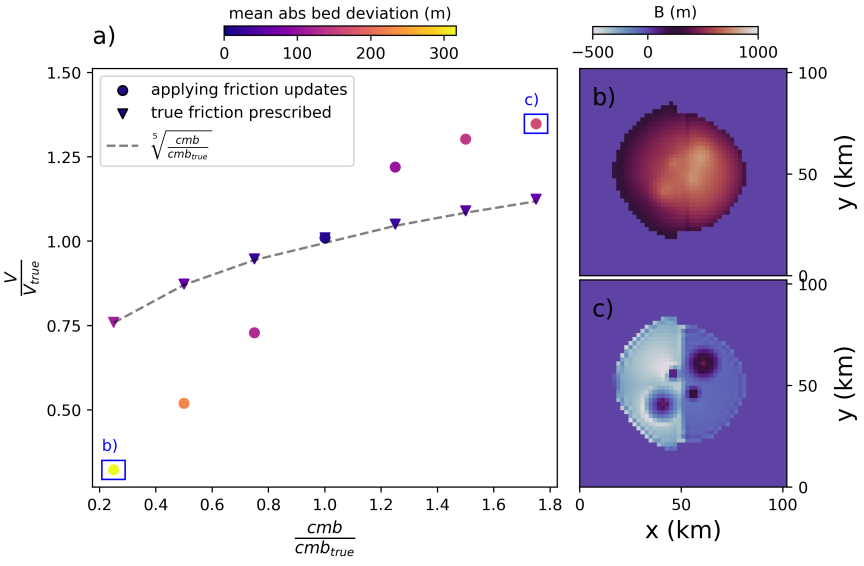

Figure A1. a) Modelled ice volume after the inversion relative to true ice volume of the ice cap as a function of mass balance perturbations. Colors indicate the mean absolute deviation between the inverted bed and the true bed. Triangles represent runs where the true friction field was prescribed from the start of the inversion, meaning that no friction updates were applied. Dots denote runs where the friction field was not known *a priori*, and therefore friction updates according to eq. (3) were applied. The dashed line is the 5th root of the mass balance errors, i.e. the theoretical relationship between mass balance and ice volume errors in the absence of friction updates; final inverted bed topography for the largest positive and negative (i.e. +-75%) mass balance perturbation when friction updates are applied shown in b) and c), respectively.

stresses, inducing smaller ice deformational velocities and hence a larger negative velocity misfit as compared to a situation with the correct friction field. This results in further updates that reduce the basal friction, thin the ice and lift up the bed. For a negative error in the 'observed' velocity, however, again an upper bound in final thickness errors is found. This is because lower observed velocities increase friction, but this is only relevant to the point until no more sliding at the base occurs. Further strengthening of the bed has no consequences, as is particularly well visible in the non-sliding (right) half of the domain where the correct bed is found even when 'observed' velocities are underestimated. As discussed previously, it is difficult to generalize the impact of these complicating effects on ice volume estimates as they depend on sliding extent and magnitude. In the case of the ice cap, we find that even a small underestimation of, say 25% of the flow velocities already results in no more sliding, thus reaching the upper ice volume error limit of about 25% volume overestimation (Fig. A2).

Furthermore, we simulate how errors in the glacier surface shape translate into bed errors. To that end, we add random noise with a standard deviation of 5 m, 10 m, 15 m, 25 m and 50 m to the ice cap surface. From theory, it is well-known that surface shape errors can lead to large bed elevation errors since bed undulations typically leave a surface expression that is only

https://doi.org/10.5194/tc-2023-43
Preprint. Discussion started: 4 April 2023

The Cryosphere Discussions

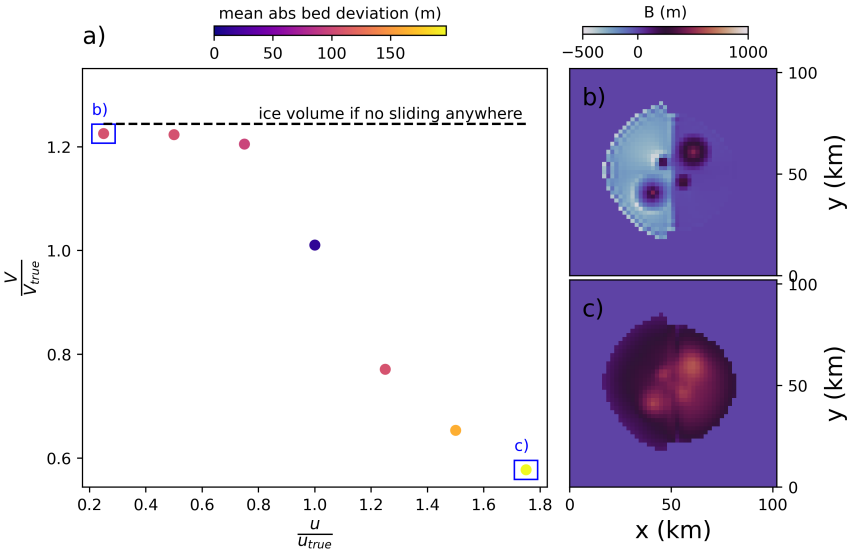

Figure A2. Modelled ice volume after the inversion relative to true ice volume of the ice cap as a function of velocity perturbations. Colors indicate the mean absolute deviation between the inverted bed and the true bed. The dashed line denotes the ice volume if the inversion is run without allowing any sliding anywhere; the final inverted bed topography for the largest positive and negative (i.e. +-75%) velocity perturbation shown in b) and c), respectively.

a fraction of their magnitude (Raymond and Gudmundsson, 2005; Habermann et al., 2012; Bahr et al., 2014). Even a small surface bump, therefore, will be interpreted as a large bed undulation by the inversion. Generally, this effect is stronger for thicker and non-sliding ice, while thin sliding ice is affected to a lesser degree. Smoothing of the input data or regularization tools (e.g. eq. (2)) can mitigate problems arising from surface noise. To show the unmitigated effects of surface noise for the purpose of this sensitivity analysis, we do not smooth the input data, and only apply the same weak regularization as in all other experiments shown here by setting the parameter $\theta = 2.5\%$ in eq. (2). Indeed, Fig. A3 demonstrates that already with little surface noise, considerable bed noise is introduced, although the general bed shape can still be seen. As predicted by theory, the sliding (left) half of the domain is less affected than the non-sliding right half. For large surface noise, the bed shape is essentially unrecognizable, as is exemplified by a mean absolute bed deviation above 200. However, Fig. A3 also shows that the modelled ice cap volume is largely unaffected by surface noise, as is expected when the mass flux through the domain and the reference velocity field are unaltered.

Next, we consider ice temperature errors (Fig. A4). Specifically, we change the ice temperature from its true value (used to build the ice cap) of 268 K to values of 264 K, 266 K, 270 K and 272 K. With the isothermal flow law used here, this means that the ice is uniformly made stiffer or softer as compared to its true viscosity. Colder ice deforms less, and so a thicker ice

https://doi.org/10.5194/tc-2023-43
Preprint. Discussion started: 4 April 2023

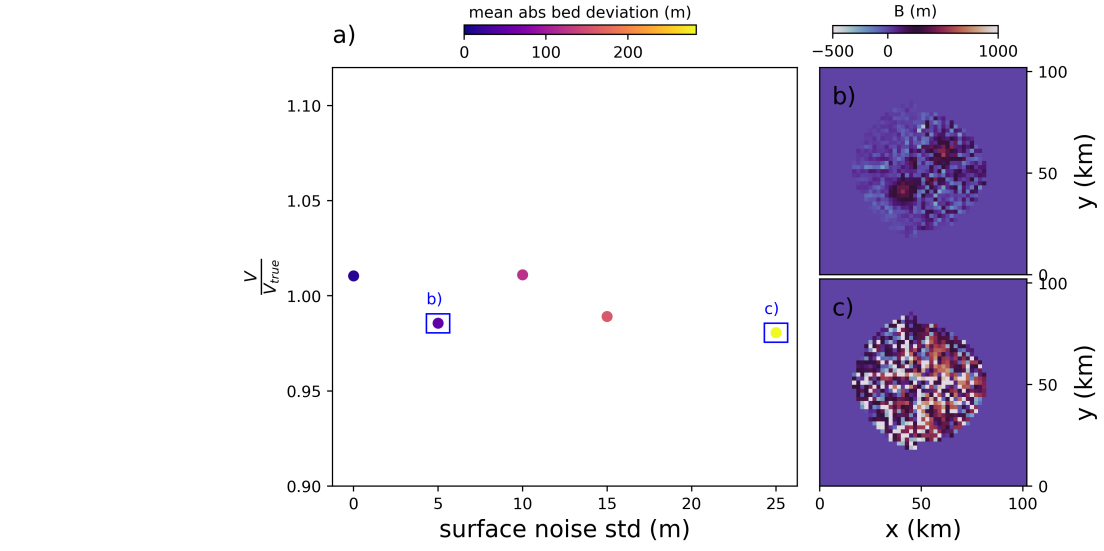

Figure A3. Modelled ice volume after the inversion relative to true ice volume as a function of surface shape perturbations with random noise. Colors indicate the mean absolute deviation between the inverted bed and the true bed; final inverted bed topography for the smallest and largest surface shape perturbation shown in b) and c), respectively.

cap can be expected from a negative ice temperature error, whereas the opposite is the case for a positive ice temperature error. However, the results of the perturbation analysis suggest that this is not the case. Rather, only small errors in final ice volume below 10% are introduced by perturbing ice temperature. This is because the friction updates compensate for too stiff or too soft ice by reducing the subglacial friction if the ice is too slow, thinning the glacier, or by increasing friction if the ice is too fast (again, however, if there is no sliding at all, this does not have any effect). Indeed, when prescribing the true friction field at the start of the inversion and not applying any updates to it, larger errors in final ice volume are apparent for both too cold and too warm ice, as compared to when friction updates were enabled (Fig. A4).

A2 Inversion parameters

We now investigate how different parameter choices for the inversion influence results. We first look at different values for the length dt of the ice-flow forward simulation. We explore values of 1 yr, 0.5 yr, 0.25 yr, 0.15 yr, 0.05 yr, 0.025 yr and 0.01 yr. Our results show virtually no difference in the final bed shape or remaining bed misfit (fig. A5), such that using small values for dt can be used to save computational time.

Furthermore, we investigate different values for the relaxation parameter β in eq. (1) (Fig. A6). β scales the dh/dt misfit into bed corrections. If β is large, the inversion should progress faster, but smaller bed features might not be resolved since

https://doi.org/10.5194/tc-2023-43
Preprint. Discussion started: 4 April 2023

The Cryosphere Discussions
Open Access
EGU

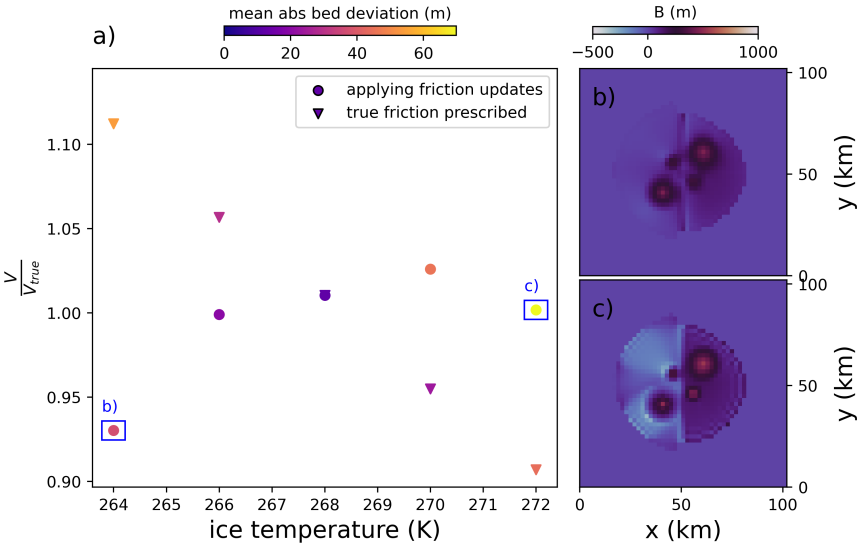

Figure A4. Modelled ice volume after the inversion relative to true ice volume of the ice cap as a function of ice temperature perturbations. Colors indicate the mean absolute deviation between the inverted bed and the true bed. Triangles represent runs where the true friction field was prescribed from the start of the inversion, meaning that no friction updates were applied. Dots denote runs where the friction field was not known *a priori*, and therefore friction updates according to eq. (3) were applied; the final inverted bed topography for the largest positive and negative (i.e. 264 K and 272 K, respectively) ice temperature perturbation when friction updates are applied is shown in b) and c), respectively.

they are overcompensated, resulting in a bed oscillating around its true value during the iterations. Conversely, a small β slows down the inversion, but results in a better resolved bed. Our sensitivity experiments confirm this. Indeed, with a larger β the bed misfit (eq. (6)) is quick to converge towards a constant value after each friction update while this is substantially slower for small β. However, the final inverted bed has a larger remaining misfit for a large than for a small β (Fig. A6).

Now, we investigate different choices of the regularization parameter θ in eq. (2) (Fig. A7). As discussed previously, θ serves the purpose of both regularizing the solution as well as allowing the inversion to converge when input data and model physics otherwise cannot balance, e.g. due to errors in the input data that are not reproducible with ice-flow physics. In the presence of larger errors, a larger θ will be required, because this gives the model flexibility to accommodate these erroneous observations. The choice of θ may thus be regarded as a measure for how well the ice-flow model is deemed to be able to reproduce observations. At the same time, however, a larger θ also increases the dependence on initial conditions because it means that a larger part of the dh/dt misfit is not accommodated with bed updates, but with surface adjustments. We start by testing the regularization effect of θ by varying it without perturbing the input data. We test values of 0, 0.015, 0.05, 0.075,

https://doi.org/10.5194/tc-2023-43
Preprint. Discussion started: 4 April 2023

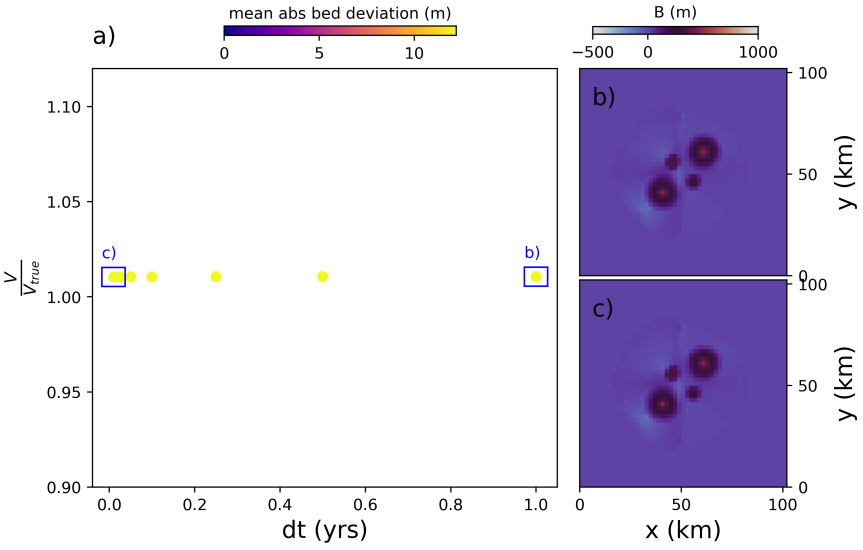

Figure A5. Modelled ice volume after the inversion relative to true ice volume of the ice cap as a function of different values for the forward modelling time step dt. Colors indicate the mean absolute deviation between the inverted bed and the true bed; the final inverted bed topography for the smallest and largest dt (i.e. 0.01 yrs and 1 yr, respectively) shown in b) and c), respectively.

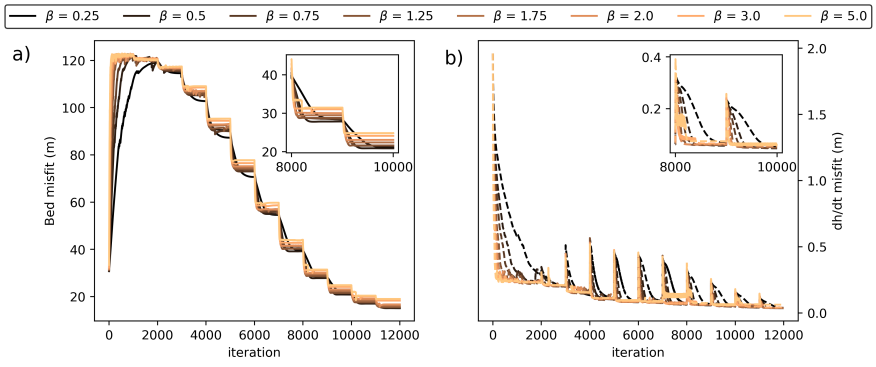

Figure A6. Sensitivity of bed inversion to the parameter β (eq. (1)). a) bed misfit per iteration step; b) dh/dt misfit per iteration step. Inset plots show zoom to iterations 8000 to 10000. Sharp steps (a) or peaks (b) occur when friction updates are applied.

0.1 and 0.3 for θ. The results show that without any surface updates (i.e. $\theta = 0$), small-scale bed irregularities are introduced to the solution. They are too small to leave any noticeable impression on ice dynamics or surface shape, and so the inversion is not wrong in producing them; from the available surface 'observations', it is impossible to tell whether these features exist

https://doi.org/10.5194/tc-2023-43
Preprint. Discussion started: 4 April 2023

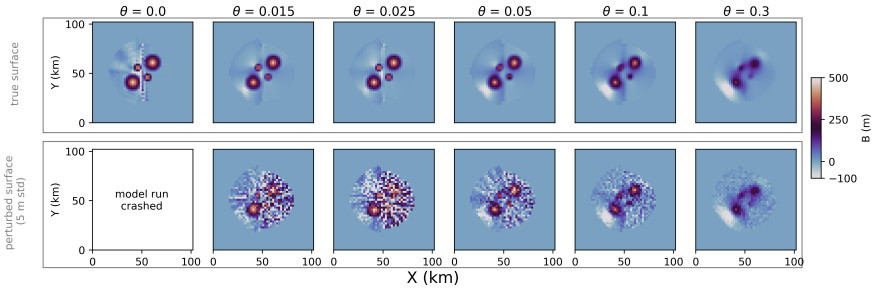

Figure A7. Final bed shape as a function of changing the regularization parameter θ. Upper row: setup without perturbed surface. Lower row: surface perturbed by adding random noise with a standard deviation of 5 m.

or not. However, it is generally undesirable to include features in the solution if they are not justified by the input data, and so regularization is in order. With increasing θ, the computed bed becomes smoother, however, this eventually comes at the cost of detail in the solution. For $\theta = 0.3$, the bed highs are no longer sharply visible. Next, we test how different choices of θ influence the inverted bed in the presence of input data errors. We investigate this here by applying the different values for θ on our ice cap where the surface shape was perturbed by adding random noise with a standard deviation of 5 m. In this case, the forward model crashes since it cannot accommodate the perturbed surface shape if $\theta = 0$, whereas increasing θ helps eliminating some of the surface noise. Again, though, when θ is too large, the bed is smooth, but also largely devoid of its characteristic topographic highs (Fig. A7). Note that the computed ice volume is always within 1% of the true ice volume regardless of θ.

Finally, we also test whether a different initial bed guess influences the results. To that end, we assume that the ice thickness is zero everywhere in the domain at the start of the inversion. We find that this has no significant impact on the recovered bed (not shown). Likewise, a different initial guess for the friction field (namely, we assume that it is slippery everywhere), does not change the bed solution. This suggests that our inversion is relatively stable towards initial conditions, although this is dependent on the choice of θ as described above.

Author contributions. TF and WvP developed the inversion methodology. TF conducted the experiments with significant input from WvP. JK provided and compiled data for the Kronebreen experiments, including processing of Pléiades imagery for generation of the 2020 DEM. TF wrote the manuscript and created the figures with significant input from WvP and JK.

Competing interests. The authors declare that they have no known competing financial interests or personal relationships that could have appeared to influence the work reported in this paper.

https://doi.org/10.5194/tc-2023-43
Preprint. Discussion started: 4 April 2023

530 *Acknowledgements.* We thank the PISM developers, in particular Constantine Khrulev, but also Ed Bueler and Andy Aschwanden for collaboration on changes to the PISM source code to speed up the inversion, for fruitful discussions and for their hospitality. TF was supported by the Swedish Research Council (VR grant 2020-04319). WvP acknowledges funding from the Swedish National Space Agency (grant 189/18). The Pléiades stereo-pairs used to generate the 2014 and 2020 DEMs used in this study were provided by the Pléiades Glacier Observatory initiative of the French Space Agency (CNES).

https://doi.org/10.5194/tc-2023-43
Preprint. Discussion started: 4 April 2023

References

Bahr, D. B., Meier, M. F., and Peckham, S. D.: The physical basis of glacier volume-area scaling, Journal of Geophysical Research: Solid Earth, 102, 20 355–20 362, https://doi.org/10.1029/97JB01696, 1997.

Bahr, D. B., Pfeffer, W. T., and Kaser, G.: Glacier volume estimation as an ill-posed inversion, Journal of Glaciology, 60, 922–934, https://doi.org/10.3189/2014JoG14J062, 2014.

Blatter, H.: Velocity and stress fields in grounded glaciers: a simple algorithm for including deviatoric stress gradients, Journal of Glaciology, 41, 333–344, https://doi.org/10.3189/S002214300001621X, 1995.

Bogorodsky, V. V., Bogorodskiĭ, V. V., Bentley, C. R., and Gudmandsen, P. E.: Radioglaciology, Springer Science & Business Media, 1985.

Brinkerhoff, D. J., Aschwanden, A., and Truffer, M.: Bayesian Inference of Subglacial Topography Using Mass Conservation, Frontiers in Earth Science, 4, 8, https://doi.org/10.3389/feart.2016.00008, 2016.

Bueler, E. and Brown, J.: Shallow shelf approximation as a "sliding law" in a thermomechanically coupled ice sheet model, Journal of Geophysical Research: Earth Surface, 114, https://doi.org/10.1029/2008JF001179, 2009.

Chen, J. and Ohmura, A.: Estimation of Alpine glacier water resources and their change since the 1870s, IAHS publ, 193, 127–135, 1990.

Chen, W., Yao, T., Zhang, G., Li, F., Zheng, G., Zhou, Y., and Xu, F.: Towards ice-thickness inversion: an evaluation of global digital elevation models (DEMs) in the glacierized Tibetan Plateau, The Cryosphere, 16, 197–218, https://doi.org/10.5194/tc-16-197-2022, 2022.

Christianson, K., Kohler, J., Alley, R. B., Nuth, C., and Van Pelt, W. J.: Dynamic perennial firn aquifer on an Arctic glacier, Geophysical Research Letters, 42, 1418–1426, 2015.

Clarke, G. K. C., Anslow, F. S., Jarosch, A. H., Radić, V., Menounos, B., Bolch, T., and Berthier, E.: Ice Volume and Subglacial Topography for Western Canadian Glaciers from Mass Balance Fields, Thinning Rates, and a Bed Stress Model, Journal of Climate, 26, 4282–4303, https://doi.org/10.1175/JCLI-D-12-00513.1, 2013.

Cuffey, K. M. and Paterson, W. S. B.: The physics of glaciers, Butterworth-Heinemann, Amsterdam, 2010.

Deschamps-Berger, C., Nuth, C., Pelt, W. V., Berthier, E., Kohler, J., and Altena, B.: Closing the mass budget of a tidewater glacier: the example of Kronebreen, Svalbard, Journal of Glaciology, 65, 136–148, https://doi.org/10.1017/jog.2018.98, 2019.

Farinotti, D., Huss, M., Bauder, A., Funk, M., and Truffer, M.: A method to estimate the ice volume and ice-thickness distribution of alpine glaciers, Journal of Glaciology, 55, 422–430, https://doi.org/10.3189/002214309788816759, 2009.

Farinotti, D., Brinkerhoff, D. J., Clarke, G. K. C., Fürst, J. J., Frey, H., Gantayat, P., Gillet-Chaulet, F., Girard, C., Huss, M., Leclercq, P. W., Linsbauer, A., Machguth, H., Martin, C., Maussion, F., Morlighem, M., Mosbeux, C., Pandit, A., Portmann, A., Rabatel, A., Ramsankaran, R., Reerink, T. J., Sanchez, O., Stentoft, P. A., Singh Kumari, S., van Pelt, W. J. J., Anderson, B., Benham, T., Binder, D., Dowdeswell, J. A., Fischer, A., Helfricht, K., Kutuzov, S., Lavrentiev, I., McNabb, R., Gudmundsson, G. H., Li, H., and Andreassen, L. M.: How accurate are estimates of glacier ice thickness? Results from ITMIX, the Ice Thickness Models Intercomparison eXperiment, The Cryosphere, 11, 949–970, https://doi.org/10.5194/tc-11-949-2017, 2017.

Farinotti, D., Brinkerhoff, D. J., Fürst, J. J., Gantayat, P., Gillet-Chaulet, F., Huss, M., Leclercq, P. W., Maurer, H., Morlighem, M., Pandit, A., Rabatel, A., Ramsankaran, R., Reerink, T. J., Robo, E., Rouges, E., Tamre, E., van Pelt, W. J. J., Werder, M. A., Azam, M. F., Li, H., and Andreassen, L. M.: Results from the Ice Thickness Models Intercomparison eXperiment Phase 2 (ITMIX2), Frontiers in Earth Science, 8, https://doi.org/10.3389/feart.2020.571923, 2021.

Flowers, G. E. and Clarke, G. K. C.: Surface and bed topography of Trapridge Glacier, Yukon Territory, Canada: digital elevation models and derived hydraulic geometry, Journal of Glaciology, 45, 165–174, https://doi.org/10.3189/S0022143000003142, 1999.

https://doi.org/10.5194/tc-2023-43
Preprint. Discussion started: 4 April 2023

Fretwell, P., Pritchard, H. D., Vaughan, D. G., Bamber, J. L., Barrand, N. E., Bell, R., Bianchi, C., Bingham, R. G., Blankenship, D. D., Casassa, G., Catania, G., Callens, D., Conway, H., Cook, A. J., Corr, H. F. J., Damaske, D., Damm, V., Ferraccioli, F., Forsberg, R., Fujita, S., Gim, Y., Gogineni, P., Griggs, J. A., Hindmarsh, R. C. A., Holmlund, P., Holt, J. W., Jacobel, R. W., Jenkins, A., Jokat, W., Jordan, T., King, E. C., Kohler, J., Krabill, W., Riger-Kusk, M., Langley, K. A., Leitchenkov, G., Leuschen, C., Luyendyk, B. P., Matsuoka, K., Mouginot, J., Nitsche, F. O., Nogi, Y., Nost, O. A., Popov, S. V., Rignot, E., Rippin, D. M., Rivera, A., Roberts, J., Ross, N., Siegert, M. J., Smith, A. M., Steinhage, D., Studinger, M., Sun, B., Tinto, B. K., Welch, B. C., Wilson, D., Young, D. A., Xiangbin, C., and Zirizzotti, A.: Bedmap2: improved ice bed, surface and thickness datasets for Antarctica, The Cryosphere, 7, 375–393, https://doi.org/10.5194/tc-7-375-2013, 2013.

Frey, H., Machguth, H., Huss, M., Huggel, C., Bajracharya, S., Bolch, T., Kulkarni, A., Linsbauer, A., Salzmann, N., and Stoffel, M.: Estimating the volume of glaciers in the Himalayan-Karakoram region using different methods, The Cryosphere, 8, 2313–2333, https://doi.org/10.5194/tc-8-2313-2014, 2014.

Fürst, J. J., Gillet-Chaulet, F., Benham, T. J., Dowdeswell, J. A., Grabiec, M., Navarro, F., Pettersson, R., Moholdt, G., Nuth, C., Sass, B., Aas, K., Fettweis, X., Lang, C., Seehaus, T., and Braun, M.: Application of a two-step approach for mapping ice thickness to various glacier types on Svalbard, The Cryosphere, 11, 2003–2032, https://doi.org/10.5194/tc-11-2003-2017, 2017.

Gantayat, P., Kulkarni, A. V., and Srinivasan, J.: Estimation of ice thickness using surface velocities and slope: case study at Gangotri Glacier, India, Journal of Glaciology, 60, 277–282, https://doi.org/10.3189/2014JoG13J078, 2014.

Glen, J. W.: The creep of polycrystalline ice, Proceedings of the Royal Society of London. Series A. Mathematical and Physical Sciences, 228, 519–538, 1955.

Gudmundsson, G. H.: Transmission of basal variability to a glacier surface, Journal of Geophysical Research: Solid Earth, 108, https://doi.org/10.1029/2002JB002107, 2003.

Habermann, M., Maxwell, D., and Truffer, M.: Reconstruction of basal properties in ice sheets using iterative inverse methods, Journal of Glaciology, 58, 795–808, https://doi.org/10.3189/2012JoG11J168, 2012.

Haeberli, W. and Hoelzle, M.: Application of inventory data for estimating characteristics of and regional climate-change effects on mountain glaciers: a pilot study with the European Alps, Annals of Glaciology, 21, 206–212, https://doi.org/10.3189/S0260305500015834, 1995.

Heining, C.: Velocity field reconstruction in gravity-driven flow over unknown topography, Physics of Fluids, 23, 032 101, https://doi.org/10.1063/1.3559144, 2011.

How, P., Benn, D. I., Hulton, N. R. J., Hubbard, B., Luckman, A., Sevestre, H., van Pelt, W. J. J., Lindbäck, K., Kohler, J., and Boot, W.: Rapidly changing subglacial hydrological pathways at a tidewater glacier revealed through simultaneous observations of water pressure, supraglacial lakes, meltwater plumes and surface velocities, The Cryosphere, 11, 2691–2710, https://doi.org/10.5194/tc-11-2691-2017, 2017.

Hugonnet, R., McNabb, R., Berthier, E., Menounos, B., Nuth, C., Girod, L., Farinotti, D., Huss, M., Dussaillant, I., Brun, F., and Kääb, A.: Accelerated global glacier mass loss in the early twenty-first century, Nature, 592, 726–731, https://doi.org/10.1038/s41586-021-03436-z, 2021.

Huss, M. and Farinotti, D.: Distributed ice thickness and volume of all glaciers around the globe, Journal of Geophysical Research: Earth Surface, 117, https://doi.org/10.1029/2012JF002523, 2012.

Kamb, B. and Echelmeyer, K. A.: Stress-Gradient Coupling in Glacier Flow: I. Longitudinal Averaging of the Influence of Ice Thickness and Surface Slope, Journal of Glaciology, 32, 267–284, https://doi.org/10.3189/S0022143000015604, 1986.

Köhler, A., Petlicki, M., Lefeuvre, P.-M., Buscaino, G., Nuth, C., and Weidle, C.: Contribution of calving to frontal ablation quantified from seismic and hydroacoustic observations calibrated with lidar volume measurements, The Cryosphere, 13, 3117–3137, https://doi.org/10.5194/tc-13-3117-2019, 2019.

Langhammer, L., Grab, M., Bauder, A., and Maurer, H.: Glacier thickness estimations of alpine glaciers using data and modeling constraints, The Cryosphere, 13, 2189–2202, https://doi.org/10.5194/tc-13-2189-2019, 2019.

Li, H., Ng, F., Li, Z., Qin, D., and Cheng, G.: An extended "perfect-plasticity" method for estimating ice thickness along the flow line of mountain glaciers, Journal of Geophysical Research: Earth Surface, 117, https://doi.org/https://doi.org/10.1029/2011JF002104, 2012.

Lindbäck, K., Kohler, J., Pettersson, R., Nuth, C., Langley, K., Messerli, A., Vallot, D., Matsuoka, K., and Brandt, O.: Subglacial topography, ice thickness, and bathymetry of Kongsfjorden, northwestern Svalbard, Earth System Science Data, 10, 1769–1781, https://doi.org/10.5194/essd-10-1769-2018, 2018.

Linsbauer, A., Paul, F., Hoelzle, M., Frey, H., and Haeberli, W.: The Swiss Alps without glaciers – a GIS-based modelling approach for reconstruction of glacier beds, Proceedings of Geomorphometry, pp. 243–247, https://doi.org/10.5167/uzh-27834, 2009.

Linsbauer, A., Paul, F., and Haeberli, W.: Modeling glacier thickness distribution and bed topography over entire mountain ranges with GlabTop: Application of a fast and robust approach, Journal of Geophysical Research: Earth Surface, 117, https://doi.org/10.1029/2011JF002313, 2012.

Luckman, A., Benn, D. I., Cottier, F., Bevan, S., Nilsen, F., and Inall, M.: Calving rates at tidewater glaciers vary strongly with ocean temperature, Nature Communications, 6, 8566, https://doi.org/10.1038/ncomms9566, 2015.

Maussion, F., Butenko, A., Champollion, N., Dusch, M., Eis, J., Fourteau, K., Gregor, P., Jarosch, A. H., Landmann, J., Oesterle, F., Recinos, B., Rothenpieler, T., Vlug, A., Wild, C. T., and Marzeion, B.: The Open Global Glacier Model (OGGM) v1.1, Geoscientific Model Development, 12, 909–931, https://doi.org/10.5194/gmd-12-909-2019, 2019.

Michel, L., Picasso, M., Farinotti, D., Bauder, A., Funk, M., and Blatter, H.: Estimating the ice thickness of mountain glaciers with an inverse approach using surface topography and mass-balance, Inverse Problems, 29, 035 002, https://doi.org/10.1088/0266-5611/29/3/035002, 2013.

Millan, R., Mouginot, J., Rabatel, A., and Morlighem, M.: Ice velocity and thickness of the world's glaciers, Nature Geoscience, 15, 124–129, https://doi.org/10.1038/s41561-021-00885-z, 2022.

NASA JPL: NASADEM Merged DEM Global 1 arc second V001. 2020, distributed by NASA EOSDIS Land Processes DAAC, https://lpdaac.usgs.gov/products/nasadem_hgtv001, 2020.

Neven, A., Dall'Alba, V., Juda, P., Straubhaar, J., and Renard, P.: Ice volume and basal topography estimation using geostatistical methods and ground-penetrating radar measurements: application to the Tsanfleuron and Scex Rouge glaciers, Swiss Alps, The Cryosphere, 15, 5169–5186, https://doi.org/10.5194/tc-15-5169-2021, 2021.

Nye, J. F.: A Method of Calculating the Thicknesses of the Ice-Sheets, Nature, 169, 529–530, https://doi.org/10.1038/169529a0, 1952.

Oppenheimer, M., Glavovic, B., Hinkel, J., van de Wal, R., Magnan, A., Abd-Elgawad, A., Cai, R., Cifuentes-Jara, M., DeConto, R., Ghosh, T., Hay, J., Isla, F., Marzeion, B., and Sebesvari, Z.: Sea Level Rise and Implications for Low-Lying Islands, Coasts and Communities, in: IPCC Special Report on the Ocean and Cryosphere in a Changing Climate, 2019.

Pattyn, F.: A new three-dimensional higher-order thermomechanical ice sheet model: Basic sensitivity, ice stream development, and ice flow across subglacial lakes, Journal of Geophysical Research: Solid Earth, 108, https://doi.org/10.1029/2002JB002329, 2003.

Pattyn, F., Schoof, C., Perichon, L., Hindmarsh, R. C. A., Bueler, E., de Fleurian, B., Durand, G., Gagliardini, O., Gladstone, R., Goldberg, D., Gudmundsson, G. H., Huybrechts, P., Lee, V., Nick, F. M., Payne, A. J., Pollard, D., Rybak, O., Saito, F., and Vieli, A.: Results of the Marine Ice Sheet Model Intercomparison Project, MISMIP, The Cryosphere, 6, 573–588, https://doi.org/10.5194/tc-6-573-2012, 2012.

Paul, F. and Linsbauer, A.: Modeling of glacier bed topography from glacier outlines, central branch lines, and a DEM, International Journal of Geographical Information Science, 26, 1173–1190, https://doi.org/10.1080/13658816.2011.627859, 2012.

Pollard, D. and DeConto, R. M.: A simple inverse method for the distribution of basal sliding coefficients under ice sheets, applied to Antarctica, The Cryosphere, 6, 953–971, https://doi.org/10.5194/tc-6-953-2012, 2012.

Rabatel, A., Sanchez, O., Vincent, C., and Six, D.: Estimation of Glacier Thickness From Surface Mass Balance and Ice Flow Velocities: A Case Study on Argentière Glacier, France, Frontiers in Earth Science, 6, 112, https://doi.org/10.3389/feart.2018.00112, 2018.

Raymond, M. J. and Gudmundsson, G. H.: On the relationship between surface and basal properties on glaciers, ice sheets, and ice streams, Journal of Geophysical Research: Solid Earth, 110, https://doi.org/10.1029/2005JB003681, 2005.

RGI Consortium: Randolph Glacier Inventory – A Dataset of Global Glacier Outlines: Version 6.0, NSIDC: National Snow and Ice Data Center, Boulder, Colorado USA, https://doi.org/10.7265/N5-RGI-60, 2017.

Rounce, D. R., Hock, R., Maussion, F., Hugonnet, R., Kochtitzky, W., Huss, M., Berthier, E., Brinkerhoff, D., Compagno, L., Copland, L., Farinotti, D., Menounos, B., and McNabb, R. W.: Global glacier change in the 21st century: Every increase in temperature matters, Science, 379, 78–83, https://doi.org/10.1126/science.abo1324, 2023.

Schellenberger, T., Dunse, T., Kääb, A., Kohler, J., and Reijmer, C. H.: Surface speed and frontal ablation of Kronebreen and Kongsbreen, NW Svalbard, from SAR offset tracking, The Cryosphere, 9, 2339–2355, https://doi.org/10.5194/tc-9-2339-2015, 2015.

Vallot, D., Pettersson, R., Luckman, A., Benn, D. I., Zwinger, T., Pelt, W. J. J. V., Kohler, J., Schäfer, M., Claremar, B., and Hulton, N. R. J.: Basal dynamics of Kronebreen, a fast-flowing tidewater glacier in Svalbard: non-local spatio-temporal response to water input, Journal of Glaciology, 63, 1012–1024, https://doi.org/10.1017/jog.2017.69, 2017.

Vallot, D., Åström, J., Zwinger, T., Pettersson, R., Everett, A., Benn, D. I., Luckman, A., van Pelt, W. J. J., Nick, F., and Kohler, J.: Effects of undercutting and sliding on calving: a global approach applied to Kronebreen, Svalbard, The Cryosphere, 12, 609–625, https://doi.org/10.5194/tc-12-609-2018, publisher: Copernicus GmbH, 2018.

van der Wel, L. G., Streurman, H. J., Isaksson, E., Helsen, M. M., Wal, R. S. W. V. D., Martma, T., Pohjola, V. A., Moore, J. C., and Meijer, H. a. J.: Using high-resolution tritium profiles to quantify the effects of melt on two Spitsbergen ice cores, Journal of Glaciology, 57, 1087–1097, https://doi.org/10.3189/002214311798843368, 2011.

van Pelt, W. J. J. and Kohler, J.: Modelling the long-term mass balance and firn evolution of glaciers around Kongsfjorden, Svalbard, Journal of Glaciology, 61, 731–744, https://doi.org/10.3189/2015JoG14J223, 2015.

van Pelt, W. J. J., Oerlemans, J., Reijmer, C. H., Pettersson, R., Pohjola, V. A., Isaksson, E., and Divine, D.: An iterative inverse method to estimate basal topography and initialize ice flow models, The Cryosphere, 7, 987–1006, https://doi.org/10.5194/tc-7-987-2013, 2013.

van Pelt, W. J. J., Pettersson, R., Pohjola, V. A., Marchenko, S., Claremar, B., and Oerlemans, J.: Inverse estimation of snow accumulation along a radar transect on Nordenskiöldbreen, Svalbard, Journal of Geophysical Research: Earth Surface, 119, 816–835, https://doi.org/10.1002/2013JF003040, 2014.

van Pelt, W. J. J., Pohjola, V., Pettersson, R., Marchenko, S., Kohler, J., Luks, B., Hagen, J. O., Schuler, T. V., Dunse, T., Noël, B., and Reijmer, C.: A long-term dataset of climatic mass balance, snow conditions, and runoff in Svalbard (1957–2018), The Cryosphere, 13, 2259–2280, https://doi.org/10.5194/tc-13-2259-2019, 2019.

https://doi.org/10.5194/tc-2023-43
Preprint. Discussion started: 4 April 2023

Welty, E., Zemp, M., Navarro, F., Huss, M., Fürst, J. J., Gärtner-Roer, I., Landmann, J., Machguth, H., Naegeli, K., Andreassen, L. M., Farinotti, D., Li, H., and GlaThiDa Contributors: Worldwide version-controlled database of glacier thickness observations, Earth System Science Data, 12, 3039–3055, https://doi.org/10.5194/essd-12-3039-2020, 2020.

Werder, M. A., Huss, M., Paul, F., Dehecq, A., and Farinotti, D.: A Bayesian ice thickness estimation model for large-scale applications, Journal of Glaciology, 66, 137–152, https://doi.org/10.1017/jog.2019.93, 2020.

Winkelmann, R., Martin, M. A., Haseloff, M., Albrecht, T., Bueler, E., Khroulev, C., and Levermann, A.: The Potsdam Parallel Ice Sheet Model (PISM-PIK) – Part 1: Model description, The Cryosphere, 5, 715–726, https://doi.org/10.5194/tc-5-715-2011, 2011.

Zorzut, V., Ruiz, L., Rivera, A., Pitte, P., Villalba, R., and Medrzycka, D.: Slope estimation influences on ice thickness inversion models: a case study for Monte Tronador glaciers, North Patagonian Andes, Journal of Glaciology, 66, 996–1005, https://doi.org/10.1017/jog.2020.64, 2020.